Dehydration Melting and Proterozoic Granite Petrogenesis in a Collisional Orogen-A Case from the Svecofennian of Southern Finland

Andersen, Tom

2021-12

Andersen , T & Ramo , O T 2021 , ' Dehydration Melting and Proterozoic Granite Petrogenesis in a Collisional Orogen-A Case from the Svecofennian of Southern Finland ' , Journal of Earth System Science , vol. 32 , no. 6 , pp. 1289-1299 . https://doi.org/10.1007/s12583-020-1385-8

http://hdl.handle.net/10138/346989
https://doi.org/10.1007/s12583-020-1385-8

acceptedVersion

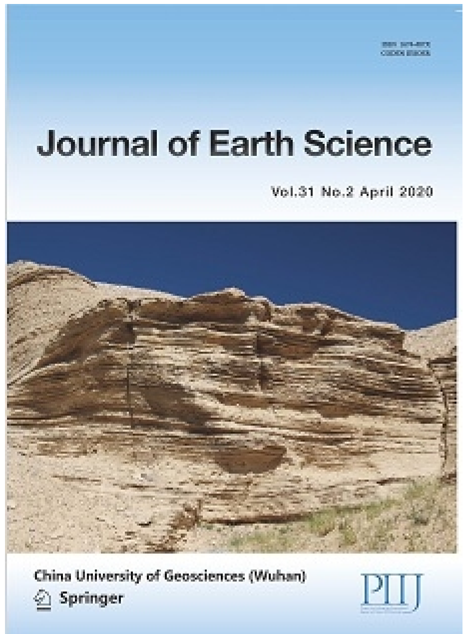

Dehydration melting and Proterozoic granite petrogenesis in a collisional orogen – a case from the Svecofennian of southern Finland

Journal:	*Journal of Earth Science*
Manuscript ID	JES-09-2020-0483.R2
Manuscript Type:	Original Article
Date Submitted by the Author:	n/a
Complete List of Authors:	Andersen, Tom; University of Oslo, Department of Geosciences Rämö, Tapani; University of Helsinki, Department of Geosciences and Geography
Keywords:	Leucogranite, rapakivi granite, anatexis

Dehydration melting and Proterozoic granite petrogenesis in a collisional orogen – a case from the Svecofennian of southern Finland

Andersen, T.[1], **Rämö, O.T.**[2]

[1]*Department of Geosciences, University of Oslo, N-0316 Oslo, Norway E-mail: tom.andersen@geo.uio.no*

[2]*Department of Geosciences and Geography, Geology and Geophysics Research Program, P.O. Box 64, 00014 University of Helsinki, Finland*

ABSTRACT: Dehydration melting of metasupracrustal rocks at mid- to deep-crustal levels can generate water undersaturated granitic melt. In this study, we evaluate the potential of ~1.89-1.88 Ga metasupracrustal rocks of the Precambrian of southern Finland as source rocks for the 1.86-1.79 Ga lateorogenic leucogranites in the region, using the rhyolite-MELTS approach (Gualda et al., 2012). Melt close in composition to leucogranite is produced over a range of realistic pressures (5 to 8 kbar) and temperatures (800 to 850 ^oC), at 20-30% of partial melting, allowing separation of melt from unmelted residue. The solid residue is a dry, enderbitic to charnoenderbitic ganulite depleted in incompatible components, and will only yield further melt above 1000-1050 ^oC, when rapidly increasing fractions of increasingly calcic (granodioritic to tonalitic) melts are formed. The solid residue after melt extraction is incapable of producing syenogranitic magmas similar to the mid-Proterozoic, A-type rapakivi granites on further heating. The granitic fraction of the syenogranitic rapakivi complexes must thus have been formed by a different chain of processes, involving mantle-derived mafic melts and melts from crustal rock types not conditioned by the preceding lateorogenic Svecofennian anatexis.

KEYWORDS Leucogranite, rapakivi granite, anatexis, restite, depleted granulite, Finland

1 INTRODUCTION

The origin of granite melts remains a controversial issue, not least because energy-conserved modeling schemes pertinent to granitic systems have not been fully developed. An important step forward in this regard was the release of the rhyolite-MELTS software (Gualda et al., 2012; Ghiorso and Gualda, 2015) that delivers a much improved prediction of the quartz-feldspar saturation surface as a function of pressure and allows control on saturation conditions of H_2O-CO_2 mixed fluids in silicate liquids. Using this approach, we have embarked upon a project to evaluate possible modes of origin of two different granite suites from the Finnish Precambrian – Paleoproterozoic peraluminous leucogranites and Paleo- to Mesoproterozoic subaluminous (ferroan) rapakivi granites.

Regarding possible crustal protoliths of granites, minerals such as muscovite and biotite, in some cases also amphibole, are important water-bearing constituents of low- to medium-grade metasupracrustal rocks. On heating at elevated pressure, these minerals will eventually break down and their water content will be liberated to a hydrous fluid phase through metamorphic devolatilization reactions or dissolve to form a water-undersaturated, aluminosilicate melt by processes known as dehydration melting (e.g., Bucher and Frey, 2002; Spear et al., 1999; Johannes and Holtz, 1996). Depending on the composition of the protolith, the melts produced will range in composition from tonalitic to granitic (Johannes and Holtz, 1996, and references therein). Dehydration melting of amphibole-bearing mafic protoliths has long been regarded as a process responsible for plagiogranite plutonism in orogenic belts (e.g., Beard and Lofgren, 1991; Wolf and Wyllie, 1994), but the process is in no way restricted to active convergent margin settings. Given a sufficient supply of thermal energy, any mica/amphibole-bearing protolith at deep to middle crustal levels will eventually reach temperature and pressure conditions where OH-bearing minerals will become unstable.

Solidus curves for water-undersaturated rock systems have positive slope in the PT space (e.g., Holtz et al., 2001). It is therefore possible to induce partial melting in the middle to lower crust both by increasing the temperature at more or less constant pressure and by decompression. Sufficient temperature increase to induce partial melting may be caused by emplacement of hot, mantle derived magma into the crust (Frost and Frost, 1987). Decompression-induced melting is possible during crustal thinning and resulting rapid uplift and exhumation of deep crust in lateorogenic collapse of orogenic belts (e.g., Vanderhaeghe et al., 1999; Crawford et al., 2009). Furthermore, radioactive decay of ^{235}U, ^{238}U, ^{232}Th and ^{40}K will cause internal heating in compositionally evolved crust with localized concentrations of heat-producing elements (e.g., Sandiford et al., 1998; Clauser, 2011), which results in anatexis of the fertile lithologic units present (Chamberlain and Sonder, 1990). Such anatexis has been suggested to lead to voluminous melt fractions (e.g., Gerdes et al., 2000; Kukkonen and Lauri, 2009).

In batch melting (e.g., Shaw, 1970), and even in a melting scenario in which melt is separated from residue quasi-continously (e.g., Bons et al., 2004) or episodically (e.g., Vigneresse, 2007), the solid residue formed in the process will be in at least local equilibrium with the melt that is extracted (e.g. Spear et al., 1999). The relationship between melting conditions (pressure, temperature), protolith composition, degree of melting and composition of the melt produced can therefore be evaluated from thermodynamical models incorporating data on relevant minerals and melt compositions. These have to be considered with the rheologic critical melt percentage (RCMP) that marks the rheology change of the anatectic system from brittle to ductile and the condition for separation of melt from residue (Arzi, 1978).

In this study, we have applied the rhyolite-MELTS software (Gualda et al., 2012, Ghiorso and Gualda 2015) to simulate partial melting processes of metasupracrustal rock types in the Palaeoproterozoic Svecofennia tectonic province of southern Finland, also studied e.g. by Kukkonen and Lauri (2009, 2016). The problems to be addressed are (1): whether or not melting of realistic metasupracrustal protoliths will produce liquids that approach the composition of the widespread ca. 1.83 Ga leucogranites in the region, emplaced subsequent to the assembly of protocontinent Fennoscandia; (2): what was the amount of melt extracted; (3): what was the nature of the solid residue left behind after melt extraction; and (4): whether or not further heating of this residue may have contributed to the ca. 1650-1540 Ma bimodal rapakivi granite magmatism in the region.

2 GEOLOGICAL SETTING

The Svecofennia tectonic province (Nironen, 2017) in southern and central Finland comprises an amalgamation of Paleoproterozoic crustal domains, assembled onto the Archean nucleus of the Fennoscandian shield by convergent processes by ~1.87 Ga (Fig. 1). Two major tectonic provinces, the Western Finland subprovince and the Southern Finland subprovince (Fig. 1) mark the bulk of the volume of the juvenile Svecofennian crust. In the Southern Finland subprovince (or Arc complex of southern Finland; cf. Korsman et al. 1997) calc-alkaline volcanic rocks, associated sedimentary sequences and synorogenic plutons are stitched together by two suites of granitoid rocks – the ~1.86-1.79 Ga lateorogenic leucogranites (Kurhila et al., 2010, 2011) and the ~1.65-1.54 Ga A-type rapakivi granites (Rämö et al., 2014, Heinonen et al., 2017, and references therein). The emplacement of the former followed the complex collisional events that had assembled protocontinent Fennoscandia by 1.87 Ga (Nironen, 2017) and was associated with transition from intraorogen extension at 1.84-1.83 Ga to late-Svecofennian collision at 1.82-1.80 Ga. The latter represent within-plate A-type magmatism with a characteristically bimodal (mafic-felsic) magmatic association (e.g., Rämö and Haapala, 2005).

2.1 Leucogranites and rapakivi granites

The lateorogenic leucogranites constitute the Svecofennian granite-migmatite zone (LSGM) of southern Finland (Ehlers et al., 1993). They are found as a discordant batholith-size intrusions (e.g., the Puruvesi pluton in the eastern part of the LSGM; Huhma, 1986), as small, relatively homogeneous bodies (a few km in diameter in general) with migmatic contacts with country rocks, and as pegmatitic segregations and flat-lying dike systems that cross-cut the earlier supracrustal and granitoid rocks (Fig. 2). In terms of volume, the leucogranite bodies are probably smaller than what may be suggested by the current exposure depicted in the geological map.

Most of the southern Finland leucogranites have SiO_2 between 70 and 75%, clustering around the liquidus minimum in the Ab-Or-Qz system (Fig. 3a). They have K_2O up to 6 wt% and are moderately peraluminous, with aluminium saturation index (ASI) around 1.1 and normative corundum between 1.0 and 2.5 %. Most of the leucogranite intrusions of the zone have crystallization ages (U-Pb on zircon and monazite) around 1.83 Ga, but the overall age range is surprisingly wide, from ~1.86 Ga to ~1.79 Ga (Kurhila et al., 2011). Zircon in the leucogranites shows a large range of Hf isotopic variation, with epsilon-Hf(t) from ca. -18 to +4, suggesting that a range of metaigneous and metasedimentary, Svecofennian rocks have been involved in their petrogenesis, the latter containing a component of Archaean detritus (Kurhila et al., 2010).

The *locus classicus* rapakivi granites of southern Finland were emplaced at least 150-250 Ma later than the leucogranites, within the upper part of the denudated Palaeoproterozoic orogenic crust. They are associated with contemporaneous mafic rocks (basaltic lavas and dikes, gabbroic rocks including anorthosite) and mark an anorogenic tectonic event with relatively extensive melting in the upper mantle and lower continental crust. The Wiborg batholith in southeastern Finland and adjacent Russia is the oldest center of rapakivi magmatism (1644-1627 Ma; Heinonen et al., 2017; see also Rämö and Mänttäri, 2015), rapakivi intrusions farther in the west (Fig. 2) and east (Lake Ladoga region, Russian Karelia) are younger (1590-1530 Ma). Zircon in the rapakivi granites shows a restricted epsilon-Hf(*t*) variation, from -4 to +4, suggesting an origin from relatively juvenile, Palaeoproterozoic source rocks, whereas the associated mafic rocks approach a depleted mantle signature at epsilon-Hf(*t*) of ca. +9 (Heinonen et al., 2010).

The rapakivi granites have a larger overall spread in SiO_2 (65 to 80 wt%) (Fig. 3) and K_2O generally between 4 and 7 wt% (Fig. 3d). They range from peraluminous (ASI ~ 1.1) to distinctly metaluminous (ASI<1, Fig. 3b). The larger range of variation is also seen in normative Ab-Or-Qz and Ab-Or-An (Fig. 3a,c).

3 METHODS

Rhyolite-MELTS (Gualda et al. 2012, Ghiorso and Gualda 2015) is an adaption of MELTS (Ghiorso and Sack, 1995) with an improved calibration for quartz and K feldspar that allows solid-melt equilibria in felsic systems at pressures up to 20 kbar to be modelled. Rhyolite-MELTS uses a Gibbs free energy minimization algorithm to estimate the amount and compositions of silicate melt and solid minerals in equilibrium in a given bulk composition as a function of temperature, pressure and oxygen fugacity. The underlying, internally consistent thermodynamical database incorporates data for minerals from Berman (1988) extended by solid solution models for minerals and data from experiments in natural silicate melts ranging from ultrabasic to silicic bulk compositions.

Calculations have been performed using the pre-compiled Ubuntu Linux version of rhyolite-MELTS release 1.0.2 (http://melts.ofm-research.org/unix.html) running in the Windows Subsystem for Linux on Windows 10 PC systems. Output ASCII files have been merged using the MELTS_Excel-Combine_tbl.xlsm template (Gualda and Ghiorso, 2015, file downloaded from https://magmasource.caltech.edu/alphamelts/-links.php#combine_tbl). Normative mineralogy was calculated using GCDkit4.0 (Janoušek et al., 2006; http://www.gcdkit.org/) and results were plotted using graphical functions in Matlab.

The compositions used as starting-points for the melting simulations span a comprehensive set of conceivable crustal lithologic units (Table 1): average felsic, intermediate and mafic metaigneous rocks (F, I and M, respectively), and metasedimentary rocks (pelite, P, and arkosite, A) from the Svecofennian belt of southern Finland, and combinations of these. The endmember compositions have been estimated from data in the rock chemistry database of the Geological Survey of Finland (Rock geochemical data of Finland, GTK 2020).The compositions in Table 1 and models presented in subsequent figures are identified by the proportions (in fractions of ten) of the F, I, M, A and P starting composition.

Modelling has been done over ranges of pressures (5 – 8 kbar) and temperatures (> 700 ^{o}C) that are considered relevant for the tectonothermal evolution of the Svecofennian domain in southern Finland (Hölttä and Heilimo, 2017, and references therein), at oxygen fugacity corresponding to the NNO buffer. In order to avoid problems with algorithm instability at and below the solidus, models have been calculated "from top to bottom", i.e. cooling a total composition under equilibrium conditions from a starting temperature above liquidus (1300 ^{o}C) to the required temperatures within the partial melting range without removal of melt or solids.

Files with the full set of results from the simulations can be found in Electronic Appendix 1 and 2.

4 RESULTS

The compositions of partial melts obtained from model calculations on all but one of the bulk compositions given in Table 1 approach the observed range of SiO_2 in the leucogranites only at temperatures above 800 ^oC, which corresponds to melt-yields of 20% or more (Fig. 4). The exception is the mafic protolith (M10), which does not yield melt with sufficient SiO_2 under any of the conditions considered here (Fig. 4c). The yield depends on starting composition (Fig. 4a). The most melt-fertile source-rocks are the metasedimentary rocks (A10: Pure arkosite, P10: Pure pelite), followed by slightly less productive felsic metavolcanic rocks (F10) and mixtures of felsic metavolcanic rocks with intermediate metavolcanic and metasedimentary endmembers (F8A2, an 8:2 mixture of felsic and arkosite endmembers, F8P2, an 8:2 mixture of felsic and pelite endmembers and F6I2P1A1, which is a 6:2:1:1 mixture of felsic metavolcanites, intermediate metavolcanics, arkosite and pelite). Melt productivity decreases moderately with increasing pressure for all of these compositions, one of which is shown as an example in Fig. 4b.

The melts produced at 800-850 ^oC (melt and residual compositions at 6 kbar, 820 ^oC are shown as examples in Fig. 5) are generally granitic, with 68-72% SiO_2 and 5 to 6% K_2O (Fig. 5a,c) and with normative quartz and feldspar proportions overlapping with that of the late Svecofennian leucogranites (Fig. 5a,b). The K_2O contents of the leucogranite samples are reasonably well reproduced by all of the source-rock compositions. All the partial melts produced are peraluminous, with ASI (aluminium saturation index) ≤ 1.2 for all but the pelite endmember (P10), which yields liquids with $ASI \approx 1.8$, and the F8P2 mixture at ASI=1.5, both of which are significantly more peraluminous than the leucogranites (Fig. 5c).

The modal compositions of the residues coexisting with melt correspond to dry, granulite-facies rocks, all of which contain plagioclase and orthopyroxene as major minerals, and all but that of the mafic metavolcanic protolith contain quartz (illustrated at 6 kbar, 820 ^oC in Fig. 6). The modal quartz content amounts to 26% in the arkosite residual at 6 kbar, 820 °C, and less in the others. Clinopyroxene is found in the mafic and intermediate metavolcanic systems and in the mixture involving the mafic component (F6I2M2). Garnet is present in the mafic and metasedimentary systems, and potassium feldspar in the metasedimentary (P10, A10) and intermediate (I10) systems, and in mixtures involving these (F6I2A1P1, F8P2, F8A2). None of the solid assemblages contain muscovite or biotite, and apatite is only present in small amounts in the residuals from melting of mafic and intermediate metavolcanic protoliths. With the exception of the residual in the arkosite system (A10), which has a charnockitic modal composition, the solid residuals shown in Fig. 6 classify as enderbites or charnoenderbites.

The solid residues are dry and depleted in the melt-forming components, most notably in K_2O and to some extent also SiO_2 (Fig. 5d). The only exception to this pattern is the arkosite protolith (A10), which is itself close to granitic in composition so that withdrawal of 20% of granitic melt does not lead to any major shift of residual composition away from the starting composition (Fig. 5). The degree of K_2O depletion increases with temperature and thus with the degree of melting (Fig. 7). In terms of normative feldspar components, this amounts to a shift away from Or towards the Ab-An join (Fig. 5b) and away from the minimum liquidus temperature area in the Ab-Or-Qz diagram (Fig. 5a). The amount of K_2O depletion is strongest in the felsic and mafic metavolcanic starting compositions ($\geq$ 50%), less so for the intermediate felsic metavolcanite and F6I2A1P1 mixture (30 to 50%), moderate (10-20%) for the metapelite, and negligible for the metaarkosite, which shows a minor increase in K_2O in residues at <800 °C (Fig. 7).

Because the residues are anhydrous, they will only yield a second batch of melt when heated to the relevant dry solidus. Rhyolite-MELTS modelling suggests that extractable amounts of second-generation melt are produced at ca. 950 °C from the arkosite residue, and at ca. 1000 °C from the pelite residue initially melted at 6 kbar and 820 °C. The residues from the other starting compositions considered, temperatures of 1050-1100 °C and higher are required (Fig. 8). Initial low-fraction, second-generation partial melts will be roughly granitic in terms of major element compositions, but will move rapidly towards granodioritic to tonalitic compositions with increasing temperature and melt fraction (Fig. 9). All except the restites in the intermediate metavolcanic system

(I10) and the F6I2M2 mixture will yield peraluminous second-generation melts (*ASI*> 1.2) that are also low in K_2O (Fig. 9).

5 DISCUSSION

The numerical experiments done in this study show that it is possible to generate granitic magma with a major element composition appropriate for the late Svecofennian leucogranites of southern Finland by partial melting of metasupracrustal protoliths in the middle to lower crust at *PT* conditions that prevailed in the southern part of the Svecofennia tectonic province after the main collisional event (amalgamation of protocontinent Fennsocandia). Overall, the evolution of the Svecofennia tectonic province probably involved several orogenic stages, including microcontinent accretion, continental collision events with intervening extension and, finally, orogenic collapse before stabilization (Lahtinen et al., 2005, 2009; Nironen, 2017). The late Svecofennian period was initiated by 1.84 Ga in southern Finland by crustal extension and associated mafic to felsic magmatism (Nironen, 2005, 2017; Pajunen et al., 2008) and is characterized by high-*T* metamorphism and crustal anatexis and resultant leucogranite magmatism. Mantle-driven thermal perturbations and decompression associated with orgenic collapse presumably were the dominant driving forces for the late Svecofennian crustal anatexis.

In a high-T,P anatectic scenario, the melting protolith seeks to minimize total interfacial energy between solid residue and melt by a process in which the generated melt penetrates melt-crystal boundaries forming a wetting angle, Θ, the value of which is governed by the balance of interfacial energies (Bulau et al., 1979; Jurewicz and Watson, 1985). If $0^o < \Theta < 60^o$, the forming melt eventually penetrates all grain edges and corners and forms an interconnected, stable network throughout the melting protolith (e.g., McKenzie, 1984). For granites, Θ has been demonstrated to be on the order of $\sim 45^o$-60^o (e.g., Jurewicz and Watson, 1985). At this wetting angle range, the contiguity (extent of solid-solid contact) of a melting protolith has to decrease to 0.15-0.2 to make the system to reach the RCMP value. In an essentially static anatectic environment, this is reached at melt fractions of > 0.5 (Miller et al., 1988).

The 20-30 % partial melting suggested by our modeling results for the generation of the Svecofennian leucogranites is well below the RCMP value of the static case. However, at high strain rates (a most likely scenario for the emplacement of the Svecofennian leucogranites; see Skyttä and Mänttäri, 2008), the RCMP may be reduced by 50% relative to the static case (see Figure 4 in Miller et al., 2008). Hence the 20-30% might be quite realistic. It is also well within the range inferred for other anatectic systems (e.g., Milord et al., 2001) and from experiments (Vielzeuf and Holloway, 1988). Segregation of such a fraction of melt from the source rock may require 1 Ma or more, which is sufficient to allow extensive equilibration with restite (Rabinowics and Vigneresse, 2004; Gerdes, 2001). A batch melting scenario is therefore more appropriate for formation of the leucogranite magmas than one involving extraction of small melt batches and disequilibrium between melts and solid residue.

Spear et al. (1999) modelled partial melting of pelitic rocks in terms of a succession of low-variance melting reactions in a simplified system (NaKFMASH). The total melt productivity during the process could be described as a combination of discrete (i.e. essentially isothermal) and continuous melting reactions, resulting in a stepwise melt productivity curve at increasing temperature (Fig. 6 in Spear et al., 1999). This is similar to the approach to leucogranite petrogenesis of Kukkonen and Lauri (2009, 2016).

When considering melting reactions independently of each other, the tendency of the whole-rock system to approach equilibrium is not taken into account. To illustrate this effect, equilibrium phase proportions in part of a rhyolite-MELTS experiment on the pelitic composition (P10, with 3% water at 8 kbar) are shown in Fig. 10. Conditions and strarting compositon have been chosen to maximize stability of biotite and muscovite, for the sake of illustration. In this system, the abundance of muscovite decreases continuously with increasing temperature and melt fraction from 600 to 740 ^{o}C, and shows an increasing rate of consumption above 700 ^{o}C. The biotite abundance decreases gradually and reaches zero at 820 ^{o}C. Although the temperatures at which muscovite and biotite finally disappear may be seen as the respective ”melting” temperatures, the two minerals have contributed to the melt over the whole temperature range from solidus (< 600 ^{o}C in this example) to their final disappearance.

At pressures between 5 and 10 kbar, ca. 20% melting is achieved in the temperature range 800 to 850 ^{o}C. This is comparable, yet a bit on the low side, of the amount of melt produced by isobaric heating and resultant dehydration of a 1:1 muscovite-biotite assemblage in the NaKFMASH system assuming no added external water, presence of vapour phase at solidus and incorporation of all water released by dehydration reactions into the forming melt (Spear et al., 1999). Melt-yields in the order of 20-25 wt% suggest that the residue after melt extraction amounts to 3.8 to 4.7 times the volume of granite produced. Residues after melt extraction in the deep to middle crust are dry granulite-facies rocks depleted in water, K_2O, and by inference also in incompatible trace elements, including the heath-producing elements U and Th. The results illustrate the fact that a dehydration melting process affects the whole phase assemblage of the rock undergoing melting, and cannot be seen as a selective breakdown process affecting only the water-bearing phases of the protolith (cf. Vielzeuf and Holloway 1988).

Kukkonen and Lauri (2009, 2016) proposed that a second episode of melting in the restitic crust of the Svecofennia tectonic province in southern Finland was responsible for the generation of the 1650-1540 Ma rapakivi granites of southern Finland. The melt productivity of the residual rocks left behind after leucogranite melt extraction is limited by their dehydrated and depleted mineralogy (Fig. 6), with heat productivity strongly reduced because of the reduced concentrations of the incompatible elements U and Th. Although a second generation of anatectic melt may be produced by continued heating after first melt extraction, temperatures above 950 ^{o}C are needed for a metaarkositic restite source, the other residues would require temperatures in the range above 1000-1050 ^{o}C and higher to yield extractable amounts of melt (Fig. 8). Small fractions of granitic magma of appropriate compositions can indeed be generated from some of the residual compositions studied at $T \geq 1050$ ^{o}C. On increasing degree of melting, however, the K_2O of the melt would decrease and the normative feldspar components of the melt develop towards granodioritic, tonalitic and quartz dioritic compositions by the time 20-25% of melt has formed. Residues after the first melting of the two metasedimentary protoliths (A10, P10) are able to yield larger quantities of anatectic magma overlapping with the range of rapakivi granites in terms of normative feldspar components, but these melts would be strongly peraluminous, with significantly higher *ASI* than observed in any of the rapakivi plutons (Fig. 9), i.e. magmas more akin to S-type than A-type granite.

Estimates of intrusive temperatures of the Fennoscandian rapakivi granites vary from < 700 ^{o}C to ca. 890 ^{o}C (Eklund and Shebanov, 1999, and references therein; Ehrlich et al., 2012; Heinonen et al., 2017). Similar A-type granitic magmas elsewhere have estimated temperatures from ca. 790 ^{o}C to 900 ^{o}C, and up to 1000 ^{o}C for the more mafic members of the association (Anderson, 1980, 1983; Creaser and White, 1991). A maximum temperature of 900 ^{o}C is thus a realistic estimate for the granitic magma compositions considered here. The ascent of an anatectic magma through the crust is a buoyancy-driven process that is near-adiabatic in nature. The dT/dP gradient of adiabatic decompression paths of a magma depends on the composition and phase proportion (Rumble, 1976). Nekvasil (1991) estimated that dT/dP < 10 ^{o}C / kbar is required to preserve the typical feldspar textures of rapakivi granites during ascent of the magma. Eklund and Shebanov (1999) suggested a quasi-isothermal path for magmas of the rapakivi plutons in Finland. Assuming a maximum temperature of ~900 ^{o}C at the level of emplacement (~2 kbar pressure), the corresponding maximum temperature of the magma at 6-8 kbar would be < 960 ^{o}C, i.e. short of what is required to generate extractible fractions of melts of realistic composition (i.e. mildly peraluminous to metaluminous syeno- monzogranite melts) from the residual compositions considered here (Fig. 8). The residue after the arkosite would generate melt at such temperature, but with impermissibly high *ASI*.

Our findings thus support a model of rapakivi petrogenesis in which local radioactive heating provides a less significant contribution to the heat budget than do mafic, mantle-derived magmas emplaced in the middle to lower crust. Our preferred interpretation is a scenario of two separate melting events, first a late Svecofennian anatectic event related to orogenic collapse, during which melt-fertile components, heat and incompatible elements were removed from the middle to lower crust by lecuogranitic magmas. In a later, and not directly related process, lithospheric extension caused partial melting in the mantle, introduction of mafic magmas into the lower crust followed by partial melting of crustal rocks that were less affected by the leucogranite melting event.

Our model is compatible with the well-established understanding of rapakivi granite petrogenesis in Fennoscandia (Rämö and Haapala, 2005, and references therein). The different, thought-provoking scenario proposed by Kukkonen and Lauri (2009, 2016) is far less realistic, at least as a major petrogenetic process for the voluminous primary melts of the *locus classicus* rapakivi granites.

6 CONCLUSIONS

Thermodynamic modelling using Rhyolite-MELTS sowtware shows that anatectic melts approximating the composition of the 1860-1790 Ma leucogranites in the Svecofennia tectonic province in southern Finland can be produced by 20-30% melting of different mixtures of Palaeoproterozoic metasupracrustal rocks of the region at 800-850 ^{o}C, 5-8 kbar. Metaigneous rocks are more important source components than metasedimentary rocks. Melt formation is best approximated by a batch melting process in which melt and minerals of the solid restite approach equilibrium. It is not a disequilibrium, fractional melting process in which water-bearing minerals in the protolith are selectively removed without equilibrating with the bulk solid residue.

The residue is a dry, melt-depleted granulite-facies rock and will not be able to produce further anatectic melt of syenogranitic to monzogranitic, mildly peraluminous to metaluminous composition unless heated above 1000-1050 ^{o}C. Moreover, in this case extractable melt fractions will be granodioritic or tonalitic, not granitic. Partial melting of such residues thus did not significantly contribute to the 1650-1540 Ma rapakivi granites of southern Finland. The latter are the results of mixing of mantle-derived magma and anatectic melts from source rocks that were unaffected by the earlier partial melting event in the region.

ACKNOWLEDGEMENTS

We thank Maria de Fatima Bitencourt and Valdecir Janasi for the invitation to submit this paper to this volume. Two anonymous reviewers gave helpful comments to the first draft of the manuscript.

Electronic Supplementary Materials: ElectronicAppendix1.pdf, ElectronicAppendix2.pdf PDF files containing results of the individual model calculations.

REFERENCES CITED

Anderson, J.L., 1980. Mineral equilibria and crystallization conditions in the late Precambrian Wolf River rapakivi massif, Wisconsin. *American Journal of Science* 280: 289–332.

Anderson, J.L., 1983. Proterozoic anorogenic granite plutonism of North America. In: L.G. Medaris, Jr., C.W. Byers, D.M. Mickelson & W.C. Shanks (Editors), Proterozoic geology. *Geological Society of America Memoir* 161: 133 - 154.

Arzi, A.A., 1978. Critical phenomena in the rheology of partially melted rocks. *Tecnonophysics* 44: 173-184.

Beard, J.S., Lofgren, G.E, 1991. Dehydration melting and water-saturated melting of basaltic and andesitic greenstones and amphibolites. *Journal of Petrology* 32: 365-401.

Berman, R.G., 1988. Internally-consistent thermodynamic data for minerals in the system Na_2O-K_2O-CaO-MgO-FeO-Fe_2O_3-Al_2O_3-SiO_2-TiO_2-H_2O-CO_2. *Journal of Petrology* 29: 445-522.

Bons, P.D., Arnold, J., Elburg, M.A., Kalda, J., Soesoo, A., van Milligen, B.P., 2004. Melt extraction and accumulation from partially molten rocks. *Lithos* 78, 25-42.

Bucher, K., Frey, M., 2002. Petrogenesis of metamorphic rocks, 7th edition. Springer Verlag, Berlin. 356.

Bulau, J.R., Waff, H., Tyburczy, J.A., 1979. Mechanical and thermodynamic constraints of fluid distribution in partial melts. *Journal of Geophysical Research* 84: 6102-6108.

Chamberlain, C.P., Sonder, L.J., 1990. Heat-producing elements and the thermal and baric patterns of metamorphic belts. *Science* 250: 763-769.

Clauser, C., 2011. Radiogenic heat production in rocks. In: Gupta, H. K., ed., Encyclopedia of Solid Earth Geophysics, Springer Science+Business Media B.V., 1018-1024.

Crawford, M.L., Klepeis, K.A., Gehrels, G.E., Lindline, J., 2009. Mid-Cretaceous–Recent crustal evolution in the central Coast orogen, British Columbia and southeastern Alaska. *Geological Society of America Special Paper* 456: 97-124.

Creaser, R.A., White, A.J.R., 1991. Yardea dacite - large-volume, high-temperature felsic volcanism from the middle Proterozoic of South Australia. *Geology* 19: 48 - 51.

Ehlers, C., Lindroos, A., Selonen, O., 1993. The late Svecofennian granite-migmatite zone of southern Finland—a belt of transpressive deformation and granite emplacement. *Precambrian Research* 64: 295–309.

Ehrlich, K., Verš, E., Kirs, J., Soesoo, A., 2012. Using a titanium-in-quartz geothermometer for crystallization temperature estimation of the Palaeoproterozoic Suursaari quartz porphyry. *Estonian Journal of Earth Science* 61: 195-204.

Eklund, O., Shebanov, A.D., 1999. The origin of rapakivi texture by sub-isothermal decompression. *Precambrian Research* 95: 129-146.

Frost, B.R., Frost, C.D., 1987. CO_2, melts and granulite metamorphism *Nature* 327: 503-506.

Gerdes, A., 2001. Magma homogenization during anatexis, ascent and/or emplacement? Constraints from the Variscan Weinsberg granites. *Terra Nova* 13: 305-312.

Gerdes, A., Wörner, G., Henk, A., 2000. Post-collisional granite generation and HT-LP metamorphism by radiogenic heating: the Variscan South Bohemian Batholith. *Journal of the Geological Society, London* 157: 577-587.

Ghiorso, M.S., Sack, R.O.,1995. Chemical mass transfer in magmatic processes IV. A revised and internally consistent thermodynamic model for the interpolation and extrapolation of liquid-solid equilibria inmagmatic systems at elevated temperatures and pressures. *Contributions to Mineralogy and Petrology* 119: 197-212.

Ghiorso M.S., Gualda G.A.R., 2015. An H_2O-CO_2 mixed fluid saturation model compatible with rhyolite-MELTS. *Contributions to Mineralogy and Petrology* 169: 53. DOI 10.0007/s00410-015-1141-8.

Gualda G.A.R., Ghiorso M.S., 2015. MELTS_Excel: A Microsoft Excel-based MELTS interface for research and teaching of magma properties and evolution. *Geochemistry, Geophysics, Geosystems* 16(1): 315-324.

Gualda, G.A.R., Ghiorso, M.S., Lemons, R.V., Carley, T.L., 2012. Rhyolite-MELTS: a Modified Calibration of MELTS Optimized for Silica-rich, Fluid-bearing Magmatic Systems. *Journal of Petrology* 53: 875-890

Heinonen, A., Rämö, O.T., Mänttäri, I., Andersen, T., Larjamo, K., 2017. Zircon as a proxy for the magmatic evolution of Proterozoic ferroan granites; the Wiborg rapakivi granite batholith, SE Finland. *Journal of Petrology* 58: 2493-2517; https://doi: 10.1093/petrology/egy014

Heinonen, A.P., Andersen, T., Rämö, O.T., 2010. Re-evaluation of Rapakivi petrogenesis: Source Constraints from the Hf Isotope Composition of Zircon in the Rapakivi Granites and Associated Mafic Rocks of Southern Finland. *Journal of Petrology* 51: 1687-1709.

Hölttä, P., Heilimo, E., 2017. Metamorphic map of Finland. *Geological Survey of Finland, Special Paper* 60: 77-128.

Holtz, F., Becker, A., Freise, M., Johannes W., 2001. The water-undersaturated and dry Qz-Ab-Or system revisited. Experimental results at very low water activities and geological implications. *Contributions to Mineralogy and Petrology* 141: 347-357.

Huhma, H., 1986. Sm-Nd, U-Pb and Pb-Pb isotopic evidence for the origin of the Early Proterozoic Svecokarelian crust in Finland. *Geological Survey of Finland Bulletin* 337: 1-52.

Janoušek, V., Farrow, C. M., Erban, V., 2006. Interpretation of whole-rock geochemical data in igneous geochemistry: introducing Geochemical Data Toolkit (GCDkit). *Journal of Petrology* 47(6): 1255-1259.

Johannes, W., Holtz, F., 1996. Petrogenesis and experimental petrology of granitic rocks. Springer Verlag, Berlin. 335.

Jurewicz, S.R., Watson, E.B., 1985. The distribution of partial melt in a granitic system: The application of liquid phase sintering theory. *Geochimica et Cosmochimica Acta* 49: 1109-1121.

Korsman, K., Koistinen, T., Kohonen, J., Wennerström, M., Ekdahl, E., Honkamo, M., Idman, H., Pekkala, Y., eds., 1997. Suomen kallioperäkartta = Berggrundskarta över Finland = Bedrock map of Finland 1:1 000 000. Espoo: Geologian tutkimuskeskus.

Kukkonen, I.T., Lauri, L.S., 2009. Modelling the thermal evolution of a collisional Precambrian orogen: High heat production migmatitic granites of southern Finland. *Precambrian Research* 168: 233-246.

Kukkonen, I.T., Lauri, L.S., 2016. Mesoproterozoic rapakivi granite magmatism in the Fennoscandian shield and adjacent areas: Role of crustal radiogenic heating. Ninth symposium on the structure, composition and evolution of the lithosphere in Fennoscandia. *Geological Survey of Finland Report* S-65: 65-66.

Kurhila, M., Andersen, T., Rämö, O.T. 2010. Diverse sources of crustal granitic magma: Lu-Hf isotope data on zircon in three Paleoproterozoic leucogranites of southern Finland. *Lithos* 115: 263-271.

Kurhila, M., Mänttäri, I., Vaasjoki, M., Rämö, O.T., Nironen, M., 2011. U–Pb geochronological constraints of the late Svecofennian leucogranites of southern Finland. *Precambrian Research* 190: 1-24.

Lahtinen, R., Korja, A., Nironen, M., 2005. Paleoproterozoic tectonic evolution. In: Lehtinen, M,. Nurmi, P.A., Rämö, O.T., eds., Precambrian Geology of Finland – Key to the Evolution of the Fennoscandian Shield. Developments in Precambrian Geology, Volume 14. Elsevier, Amsterdam, 481–531.

Lahtinen, R., Huhma, H., Kähkönen, Y., Mänttäri, I., 2009. Palaeoproterozoic sediment recycling during multiphase orogenic evolution in Fennoscandia, the Tampere and Pirkanmaa belts, Finland. *Precambrian Research* 174: 310-336.

Luukas, J., Kousa, J., Nironen, M., Vuollo, J., 2017. Major stratigraphic units in the bedrock of Finland, and an approach to tectonostratigraphic division. *Geological Survey of Finland, Special Paper* 60: 9-40.

McKenzie, D., 1984. The generation and compaction of partially molten rock. *Journal of Petrology* 25: 713-765.

Miller, C.F., Watson, E.B., Harrison, T.M., 1988. Perspectives of the source, segregation and transport of granitoid magmas. *Transactions of the Royal Society of Edinburgh: Earth Sciences* 79: 135-156.

Milord, I., Sawyer, E.W., Brown, M., 2001. Formation of diatexite migmatite and granite magma during anatexis of semi-pelitic metasedimentary rocks: and example from St. Malo, France. *Journal of Petrology* 42: 487-505.

Nekvasil, H., 1991. Ascent of felsic magmas and formation of rapakivi. *American Mineralogist* 76: 1279-1290.

Nironen, M., 2005. Proterozoic orogenic granitoid rocks. In: Lehtinen, M., Nurmi, P.A., Rämö, O.T., eds., Precambrian Geology of Finland – Key to the Evolution of the

Fennoscandian shield. Developments in Precambrian Geology, Volume 14. Elsevier, Amsterdam, 443–479.

Nironen, M., 2017. Guide to the geological map of Finland – bedrock 1:1 000 000. *Geological Survey of Finland, Special Paper* 60: 41-76.

Pajunen, M., Airo, M.-L., Elminen, T., Mänttäri, I., Niemelä, R., Vaarma, M., Wasenius, P., Wennerström, M., 2008. Tectonic evolution of the Svecofennian crust in southern Finland. *Geological Survey of Finland, Special Paper* 47: 15–160.

Rabinowics, M., Vigneresse, 2004. J.-L., 2004. Melt segregation under compaction and shear channeling: Application to granitic magma segregation in a continental crust. *Journal of Geophysical Research* 109: B4407, doi:10.1029/2002JB002372.

Rämö, O.T., Haapala, I., 2005. Rapakivi granites. In: Lehtinen, M., Nurmi, P.A., Rämö, O.T., eds., Precambrian Geology of Finland – Key to the Evolution of the Fennoscandian shield. Developments in Precambrian Geology, Volume 14. Elsevier, Amsterdam, 553-562.

Rämö, O.T., Mänttäri, I., 2015. Geochronology of the Suomenniemi rapakivi granite complex revisited: Implications of point-specific errors on zircon U-Pb and refined λ_{87} on whole-rock Rb-Sr. *Bulletin of the Geological Society of Finland* 87: 25-45; http://dx.doi.org/10.17741/bgsf/87.1.002

Rämö, O.T., Turkki, V., Mänttäri, I., Heinonen, A.P., Larjamo, K., Lahaye, Y., 2014. Age and isotopic fingerprints of some plutonic rocks in the Wiborg rapakivi granite batholith with special reference to the dark wiborgite of the Ristisaari Island. *Bulletin of the Geological Society of Finland* 86, 71-91; http://dx.doi.org/10.17741/bgsf/87.1.002

Rock geochemical data of Finland, GTK, 2020. http://tupa.gtk.fi/paikkatieto/-meta/rock_geochemical_data_of_finland.html. Geological Survey of Finland.

Rumble, D., 1976. The adiabatic gradient and adiabatic compressibility. *Carnegie Institution of Washington Year Book* 75: 65 l-65 5.

Sandiford, M., Hand, M., McLaren, S., 1998. High geothermal gradient metamorphism during thermal subsidence. *Earth and Planetary Science Letters* 163: 149-165.

Shaw, D.M., 1970. Trace element fractionation during anataxis. *Geochimica et Cosmochimica Acta* 34: 237-243.

Skyttä, P., Mänttäri, I., 2008. Structural setting of late Svecofennian granites and pegmatites in Uusimaa belt, SW Finland: Age constraints and implications for crustal evolution. *Precambrian Research* 164: 86-109.

Spear, F.S., Kohn, M.J., Cheney, J.T., 1999. *P-T* paths from anatectic pelites. *Contributions to Mineralogy and Petrology* 134: 17-32.

Vanderhaeghe, O., Burg, J.-P., Tessier, C., 1999. Exhumation of migmatites in two collapsed orogens: Canadian Cordillera and French Variscides. In: Ring, U., Lister, M.T., Willett, S.D., eds., Exhumation processes: Normal faulting, ductile flow and erosion. Geological Society of London Special Publication 154: 181-204.

Vielzeuf D., Holloway J.R., 1988. Experimental determination of the fluid-absent melting reactions in the politic system: consequences for crustal differentiation. *Contributions to Mineralogy and Petrology* 98: 257-276.

Vigneresse J.L, 2007. The role of discontinuous magma inputs in felsic magma and ore generation. *Ore Geology Reviews* 30, 181-216.

Wolf, M.B., Wyllie, P.J., 1994. Dehydration-melting of amphibolite at 10 kbar: the effects of temperature and time. *Contribution to Mineralogy and Petrology* 115: 369-383.

Table 1. Source rock and unmelted residue compositions used in modelling (source rocks: Rock geochemical data of Finland, GTK 2020)

Initial compositions, weight percent oxides

	A10	P10	M10	I10	F10	F6I2M2	F8A2	F8P2	F6I2A1P1
SiO_2	73.1	63.0	51.6	62.5	70.4	65.1	70.9	68.9	68.4
TiO_2	0.4	0.8	1.2	0.8	0.4	0.6	0.4	0.5	0.5
Al_2O_3	12.7	16.8	15.8	13.2	13.8	14.1	13.6	14.4	13.9
Fe_2O_3	3.0	7.4	10.9	8.5	4.3	6.4	4.0	4.9	5.3
MnO	0.1	0.1	0.2	0.1	0.1	0.1	0.1	0.0	0.1
MgO	0.5	2.9	5.6	3.7	1.3	2.7	1.2	1.7	1.9
CaO	1.2	1.5	9.8	4.2	2.6	4.3	2.4	2.4	2.7
Na_2O	2.7	2.5	2.9	3.4	4.3	3.8	4.0	3.9	3.7
K_2O	5.4	3.9	0.9	2.5	1.7	1.7	2.4	2.1	2.4
P_2O_5	0.1	0.1	0.2	0.2	0.1	0.2	0.1	0.1	0.1
H_2O	1.0	1.0	1.0	1.0	1.0	1.0	1.0	1.0	1.0
	100.0	100.0	100.0	100.0	100.0	100.0	100.0	99.9	100.0

Residues (R) after melt-extraction at 6 kbar, 820 ^oC, weight percent oxides

	A10R	P10R	I10R	F10R	F6I2MR	F8A2R	F8P2R	F6I2A1P1R
SiO_2	74.0	61.1	60.8	70.7	63.9	71.2	68.9	68.0
TiO_2	0.4	0.9	0.9	0.4	0.7	0.4	0.5	0.5
Al_2O_3	12.5	16.5	13.2	13.9	14.2	13.7	14.1	13.9
Fe_2O_3	3.5	9.9	11.0	5.1	7.9	4.8	6.1	6.7
MnO	0.0	0.0	0.0	0.0	0.0	0.0	0.0	0.0
MgO	0.6	3.9	4.0	1.7	3.4	1.5	2.2	2.5
CaO	1.0	1.7	4.8	2.8	4.9	2.6	2.7	2.9
Na_2O	2.7	2.9	3.8	4.6	4.2	4.4	4.5	4.2
K_2O	5.3	3.1	1.4	0.8	0.7	1.4	1.0	1.3
P_2O_5	0.0	0.0	0.0	0.0	0.0	0.0	0.0	0.0
H_2O	0.0	0.0	0.0	0.0	0.0	0.0	0.0	0.0
	100.0	100.0	100.0	100.0	100.0	100.0	100.0	100.0

Key to the compositions:
A10 = Average arkosite, P10 = Average pelite, M10 = Average mafic metavolcanic rock, I10 = Average intermediate volcanic rock, F10 = Average felsic metavolcanic rock, F6I2M2 = 6:2:2 felsic + intermediate + mafic; F8A2 = 8:2 felsic + arkosite, F8P2 = 8:2 felsic + pelite, F6I2A1P1 = 6:2:1:1 felsic + intermediate + arkosite + pelite.

Figure captions

Fig. 1: Overview map showing the main Palaeoproterozoic lithodemic units of the Svecofennia tectonic province in southern and central Finland. Adopted and slightly modified from Luukas et al. (2017). Key to abbreviations: CFGC = Central Finland granitoid complex; HämS = Häme migmatite suite; PimS = Pirkanmaa migmatite suite; LaS = Lapfors suite; VaC = Vaasa complex; TeS = Teuva suite; PiS = Pirttikylä suite. Blank areas south of the border (blue line) of the Western Finland and Southern Finland subprovinces mark late Palaeoproterozoic leucogranites, late Palaeoproterozoic to Mezoproterozoic rapakivi granites and Mesoproterozoic cratonic redbed sequences and associated dolerites. Inset shows map area relative to mainland Finland.

Fig. 2: Lithological map of southern Finland, showing the distribution of the lateorogenic Svecofennian leucogranites and mid-Proterozoic rapakivi granites amongst the synorogenic lithologic units of the Svecofennia tectonic province (cf. Fig. 1). Black lines denote major deformation zones, white blank areas denote lakes. Inset shows map area relative to mainland Finland. Modified from Fig. 1 in Kurhila et al. (2010).

Fig. 3: Compositions of leucogranites and rapakivi granites. Leucogranites are shown in blue, rapakivi granites in red. Source of data: Rock geochemical data of Finland, GTK, (2020)

a: Normative Ab-Or-Qz

b: wt % SiO_2 vs. ASI

c: Normative Ab-Or-An

d: wt% SiO_2 vs. wt% K_2O

Fig. 4: Melt yields over the whole simulation range ~700 ^oC to 1300 ^oC.

a: Different compositions as function of temperature at a constant pressure of 6 kbar.

b: Melt yield from one composition (F6I2A1P1) show as a function of *T* at P= 5, 6, 7 and 8 kbar.

c: SiO_2 content of melts formed from the protolith compositions in Table 1 at 6 kbar as a function of temperature.

Abbreviations as in Table 1.

Fig. 5: Model results compared to the range of leucogranite compositions (shaded background). In all of the diagrams, bulk compositions (source rock) are given by filled squares, melts at 6 kbar, 820 ^oC by circles and residues (in *c* and *d* only) by diamonds. Colour coding is consistent as indicated in *d*. For labels, see Table 1.

Fig. 6: Phase abundances in weight percent at 6 kbar, 820 ^oC. Minor amounts of modal apatite are only present in bulk compositions M10 and I10.

Fig. 7: Potassium depletion (as wt% K_2O in residue / wt % K_2O in total system. All residues are progressively depleted in potassium, except for the metaarkosite (A10) which shows a small increase in K_2O below ca. 800 ^oC (i.e. the melt is less potassic than the residue in this temperature interval). The grey bar at 820 ^oC is shown to connect to the panels in Fig. 5.

Fig. 8: Melt yields on further heating of melt-depleted residues formed at 6 kbar, 820 ^oC (assuming full separation of melt). All systems are anhydrous, but 100 ppm water was added to the metapelitic system (P10) at T<1020 ^oC to prevent software from malfunctioning (broken part of the curve).

Fig. 9: Second generation melts obtained by further heating of the residues of the first melt separation at 820 ^oC, 6 kbar, compared to rapakivi granite compositions shown as grey background (panels and colour coding as in Fig. 5). Diamonds represent bulk composition of the residues, the evolution of melts are shown as lines terminating (at point closest to bulk composition) at 1100 ^oC, calculated at 10 degree intervals (indicated by tick marks). The starting temperature on the curves indicated on the curves differ among the bulk compositions, and reflect the temperature where a non-zero melt

production is first seen (cf. Fig. 8), i.e. 900 ^oC for A10R, 1070 ^oC for F10R. Note that A10 is completely molten above 990 ^oC. Colour coding as in Fig. 5.

Fig. 10: Phase proportion in the low-temperature part of a numeric melting experiment of the P10 metapelite composition (Table 1) with 3% water at 8 kbar. Heavy curves give phase abundance of muscovite (Mu), biotite (Bi) and liquid (Liq) as function of temperature. Thin curves are other solid phases present in the restite (Ilm: Ilmenite, Afs: Alkali feldspar, Leu: Leucite, Qtz: Quartz, Plg: Plagioclase, Grt: Garnet, Opx: Orthopyroxene)

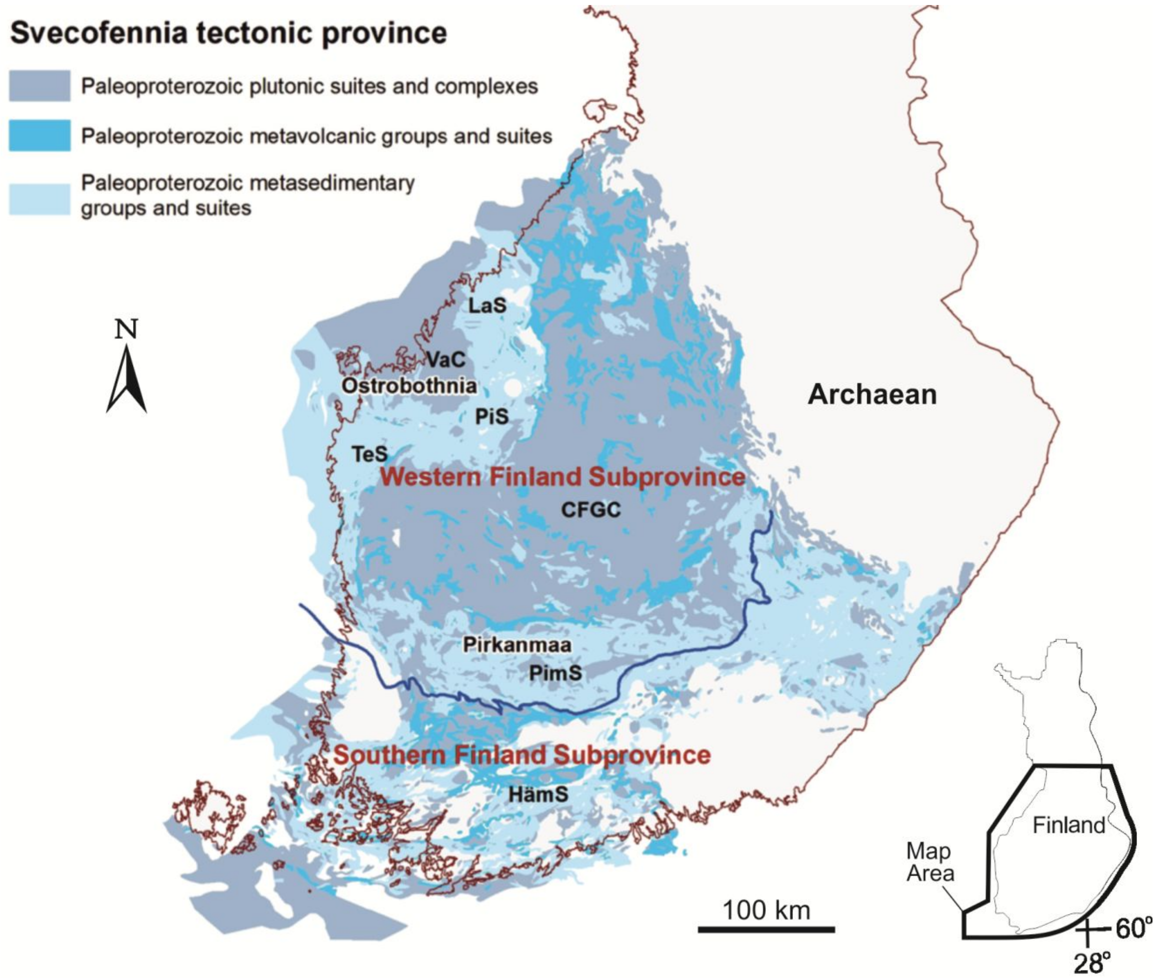

Fig. 1

30.11.202007:32:24

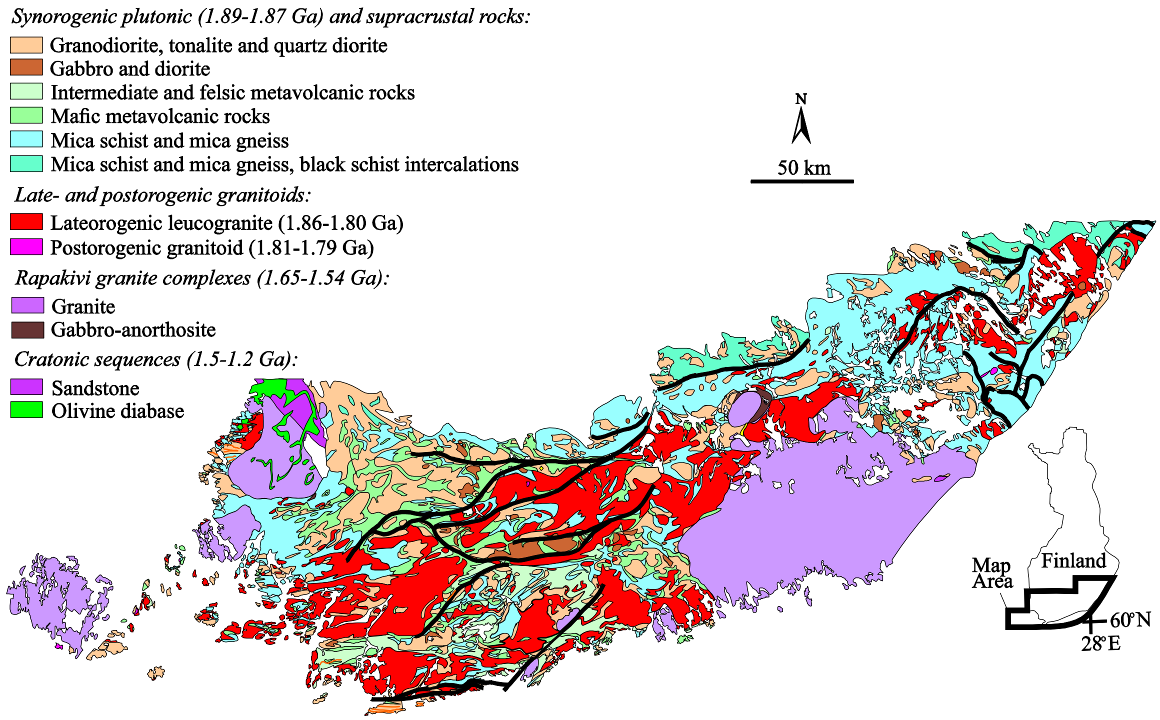
Synorogenic plutonic (1.89-1.87 Ga) and supracrustal rocks:
Granodiorite, tonalite and quartz diorite
Gabbro and diorite
Intermediate and felsic metavolcanic rocks
Mafic metavolcanic rocks
Mica schist and mica gneiss
Mica schist and mica gneiss, black schist intercalations
Late- and postorogenic granitoids:
Lateorogenic leucogranite (1.86-1.80 Ga)
Postorogenic granitoid (1.81-1.79 Ga)
Rapakivi granite complexes (1.65-1.54 Ga):
Granite
Gabbro-anorthosite
Cratonic sequences (1.5-1.2 Ga):
Sandstone
Olivine diabase
N
50 km
Map Area
Finland
60°N
28°E

Fig. 2

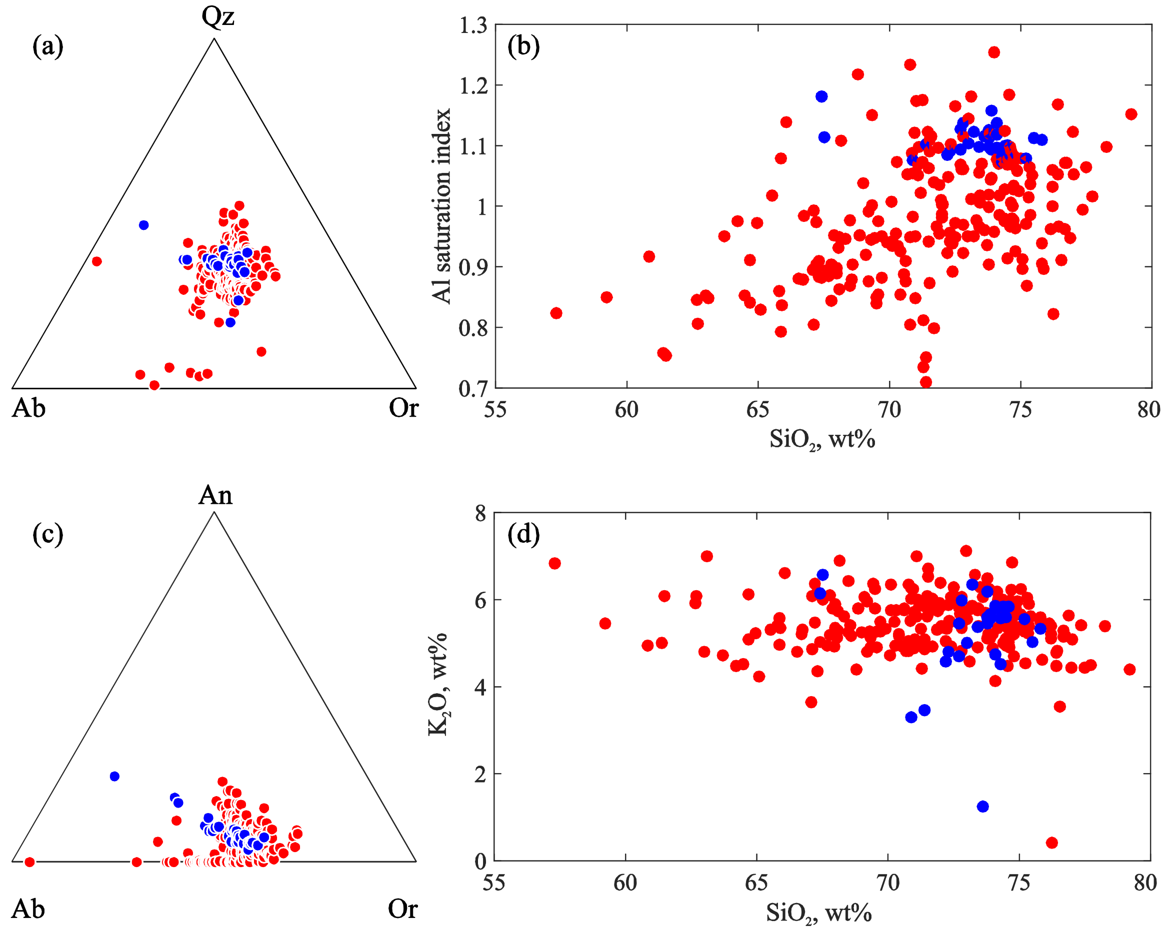

Fig. 3

30.11.202007:32:24

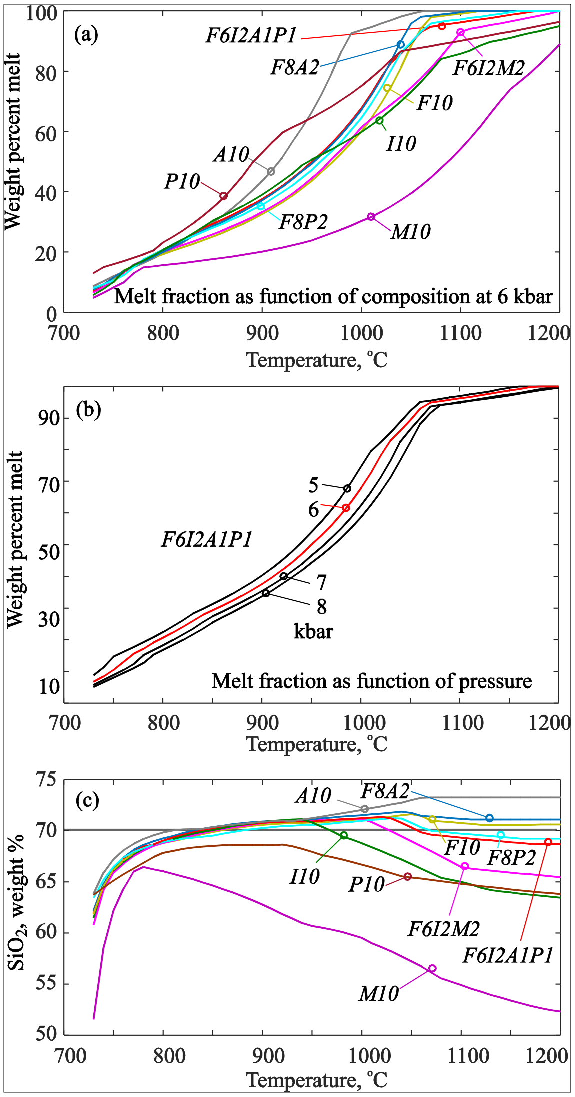
(a)
F6I2A1P1
F8A2
F6I2M2
F10
I10
A10
P10
F8P2
M10
Melt fraction as function of composition at 6 kbar
Weight percent melt
Temperature, °C
(b)
F6I2A1P1
5
6
7
8
kbar
Melt fraction as function of pressure
Weight percent melt
Temperature, °C
(c)
A10
F8A2
F10
F8P2
I10
P10
F6I2M2
F6I2A1P1
M10
SiO2, weight %
Temperature, °C

Fig. 4

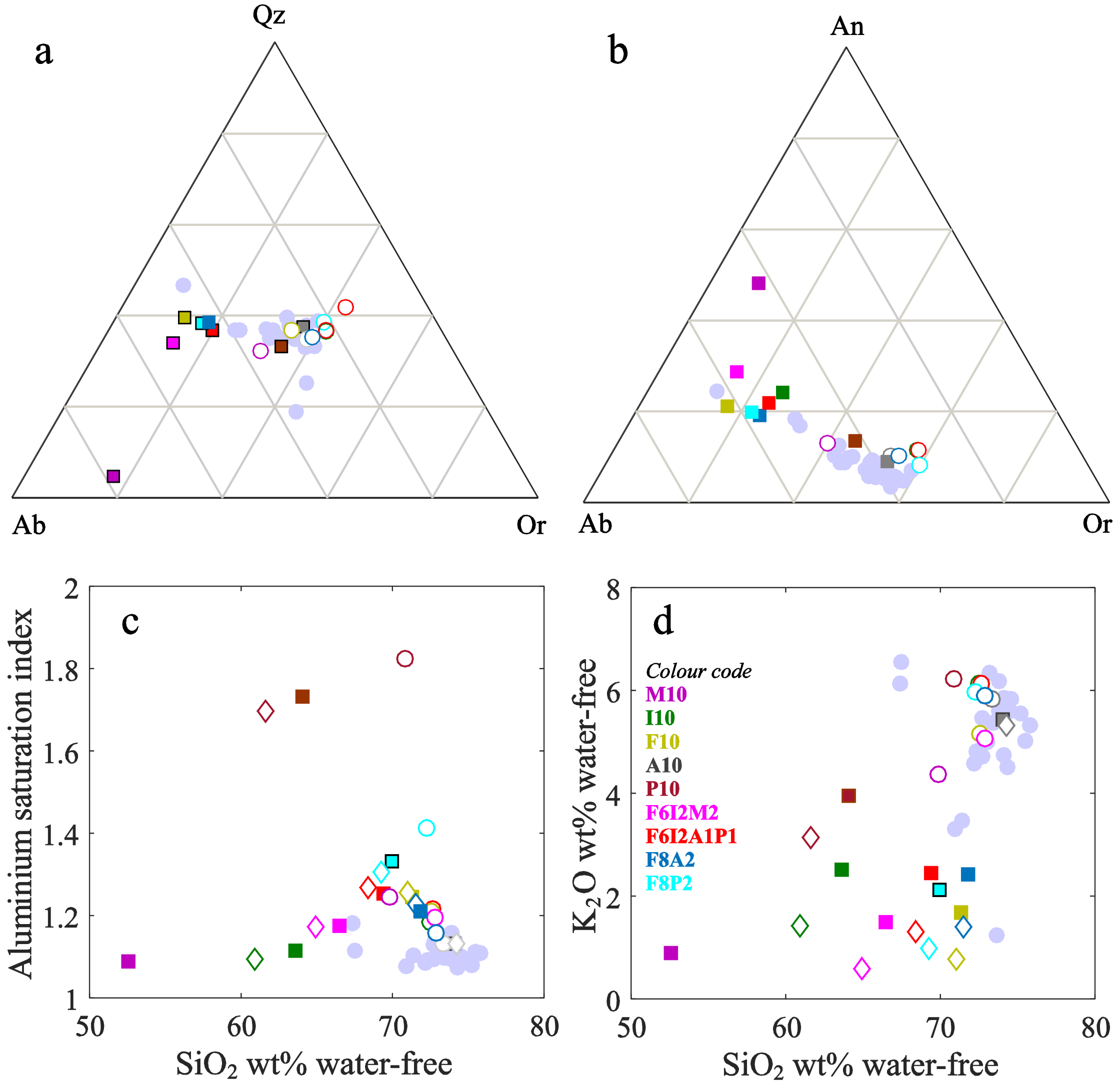
a
Qz
Ab
Or
b
An
Ab
Or
c
Aluminium saturation index
2
1.8
1.6
1.4
1.2
1
50
60
70
80
SiO2 wt% water-free
d
K2O wt% water-free
8
6
4
2
0
50
60
70
80
SiO2 wt% water-free
Colour code
M10
I10
F10
A10
P10
F6I2M2
F6I2A1P1
F8A2
F8P2

Fig. 5

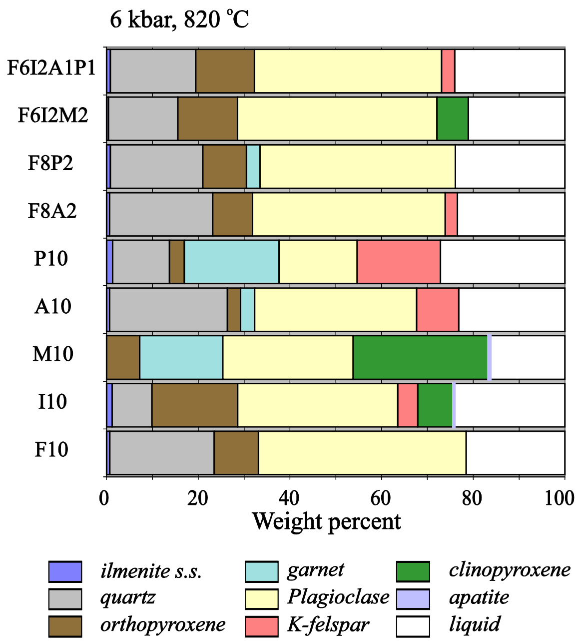

Fig. 6

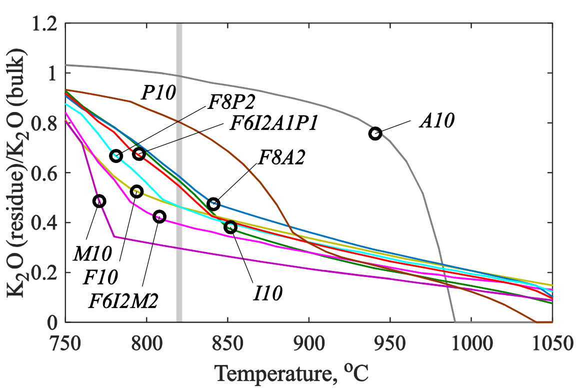

Fig. 7

30.11.202007:32:24

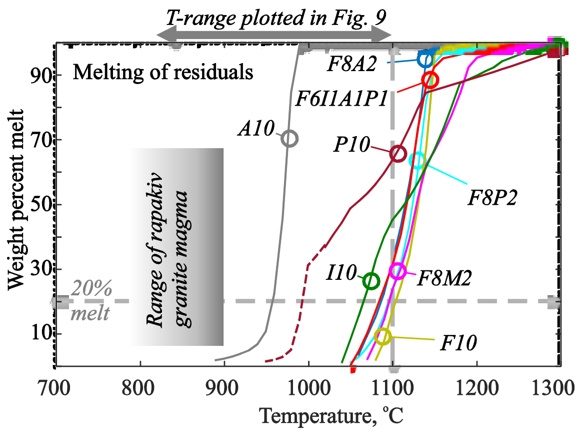
T-range plotted in Fig. 9
Melting of residuals
F8A2
F6I1A1P1
A10
P10
F8P2
Range of rapakiv granite magma
I10
F8M2
20% melt
F10
Weight percent melt
Temperature, °C
700
800
900
1000
1100
1200
1300
90
70
50
30
10

Fig. 8

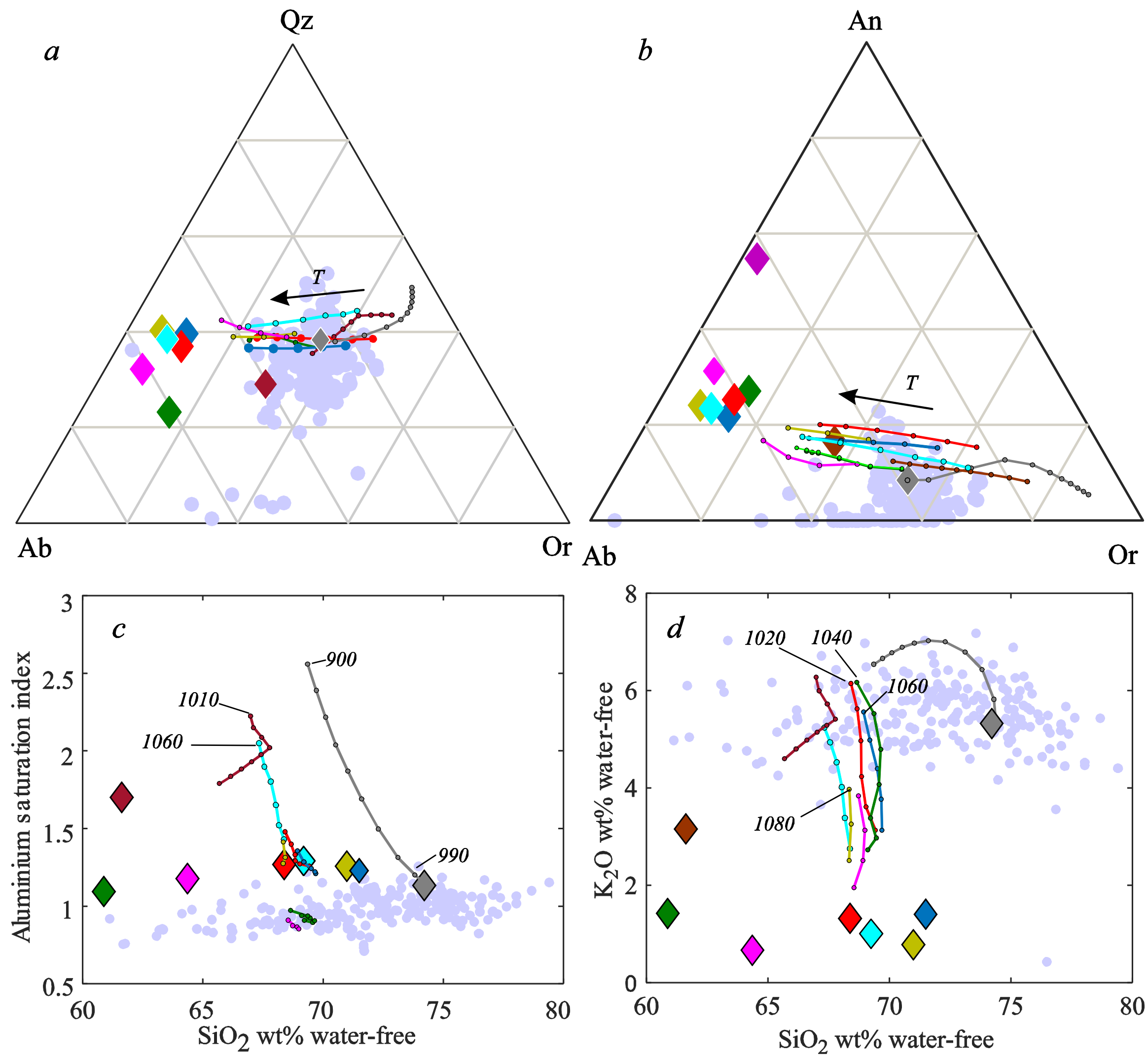

Fig. 9

30.11.202007:32:24

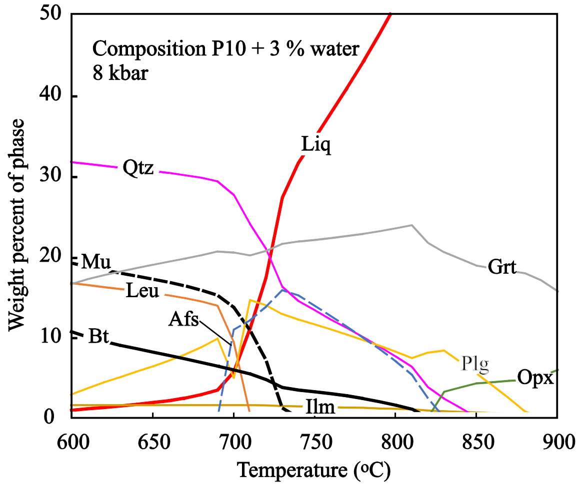

Composition P10 + 3 % water
8 kbar
Weight percent of phase
Temperature (oC)
Liq
Qtz
Mu
Leu
Afs
Bt
Grt
Plg
Opx
Ilm
0
10
20
30
40
50
600
650
700
750
800
850
900

Fig. 10

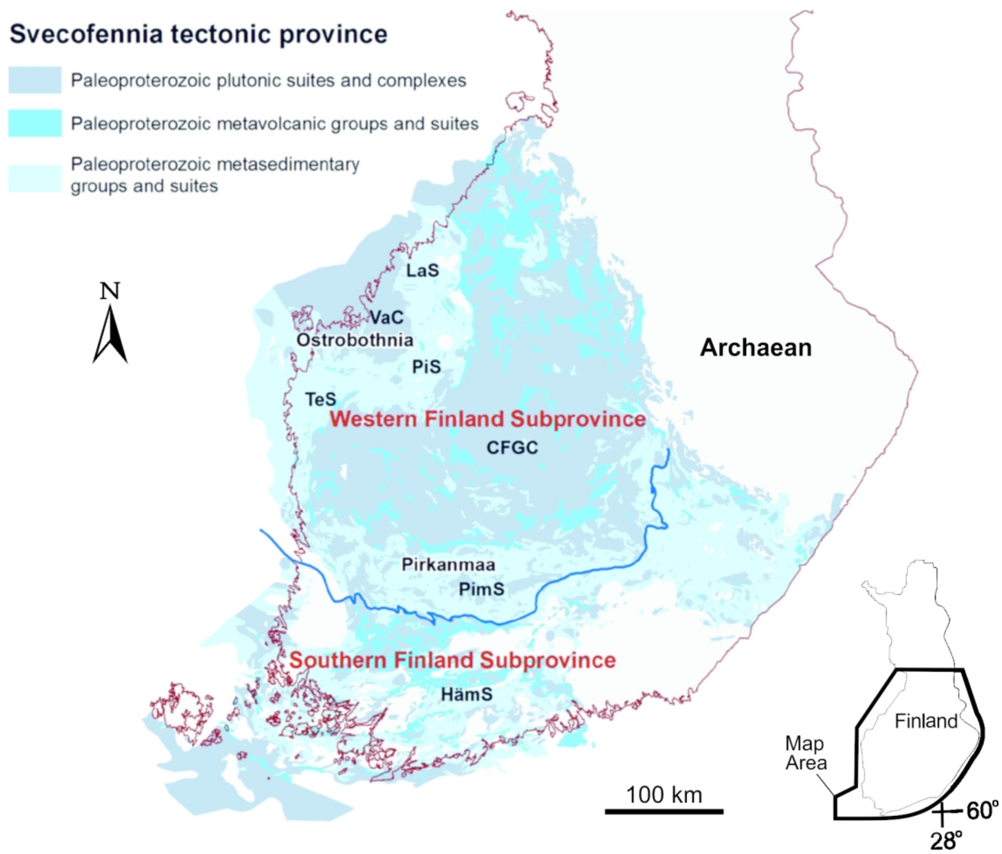

Fig. 1: Overview map showing the main Palaeoproterozoic lithodemic units of the Svecofennia tectonic province in southern and central Finland. Adopted and slightly modified from Luukas et al. (2017). Key to abbreviations: CFGC = Central Finland granitoid complex; HämS = Häme migmatite suite; PimS = Pirkanmaa migmatite suite; LaS = Lapfors suite; VaC = Vaasa complex; TeS = Teuva suite; PiS = Pirttikylä suite. Blank areas south of the border (blue line) of the Western Finland and Southern Finland subprovinces mark late Palaeoproterozoic leucogranites, late Palaeoproterozoic to Mezoproterozoic rapakivi granites and Mesoproterozoic cratonic redbed sequences and associated dolerites. Inset shows map area relative to mainland Finland.

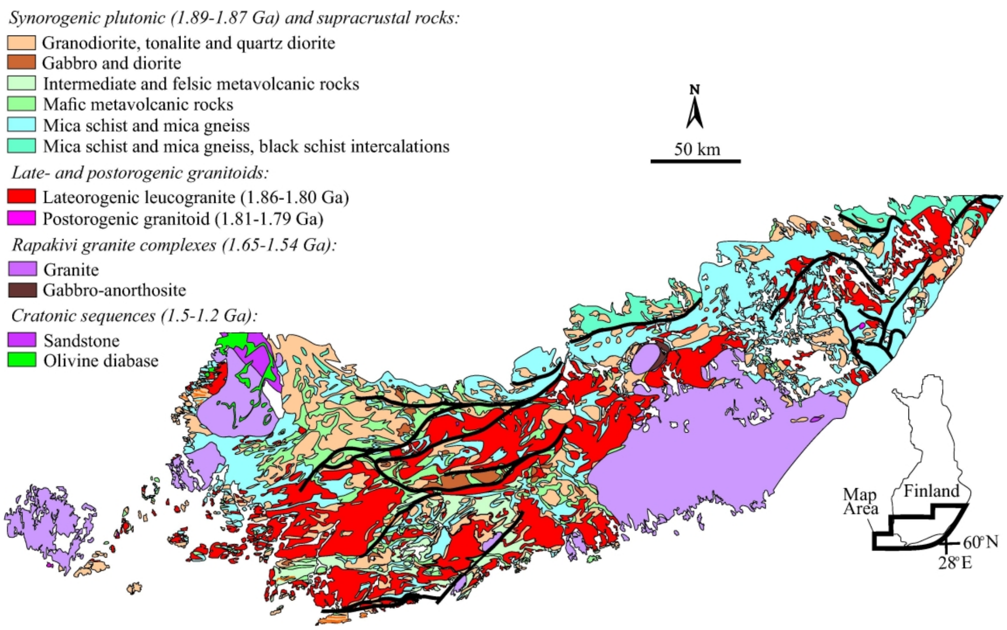

Fig. 2: Lithological map of southern Finland, showing the distribution of the lateorogenic Svecofennian leucogranites and mid-Proterozoic rapakivi granites amongst the synorogenic lithologic units of the Svecofennia tectonic province (cf. Fig. 1). Black lines denote major deformation zones, white blank areas denote lakes. Inset shows map area relative to mainland Finland. Modified from Fig. 1 in Kurhila et al. (2010).

155x95mm (600 x 600 DPI)

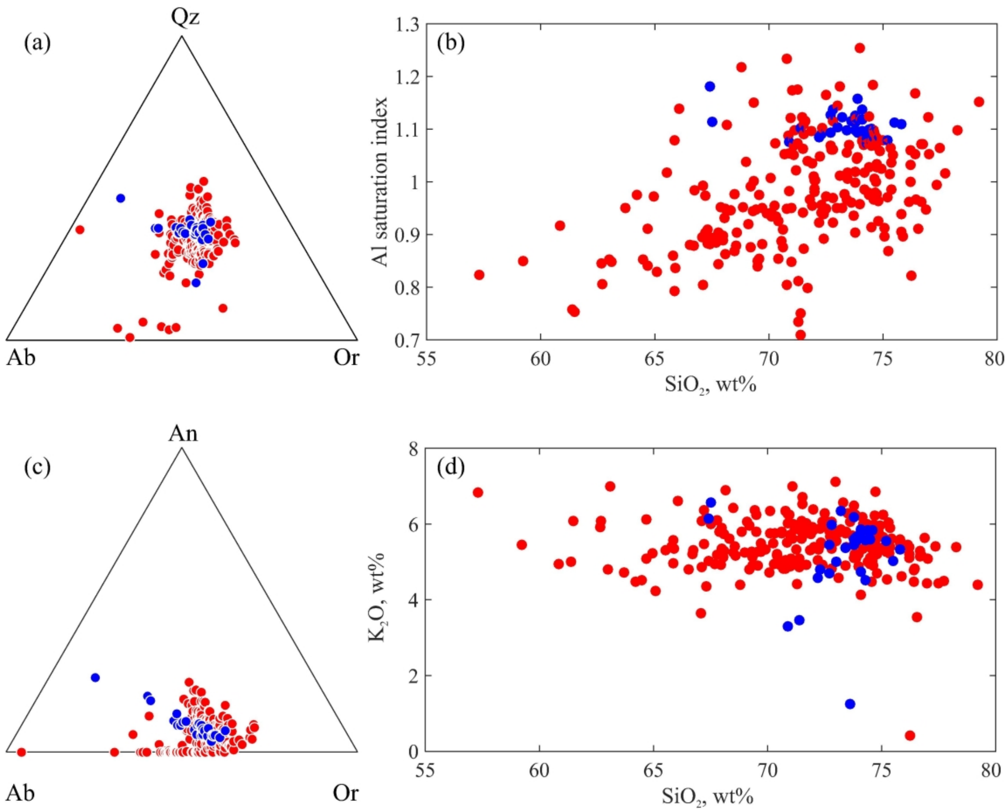

Fig. 3: Compositions of leucogranites and rapakivi granites. Leucogranites are shown in blue, rapakivi granites in red. Source of data: Rock geochemical data of Finland, GTK, (2020)

a: Normative Ab-Or-Qz

b: Normative Ab-Or-An

c: wt % SiO2 vs. ASI

d: wt% SiO2 vs. wt% K2O

155x124mm (600 x 600 DPI)

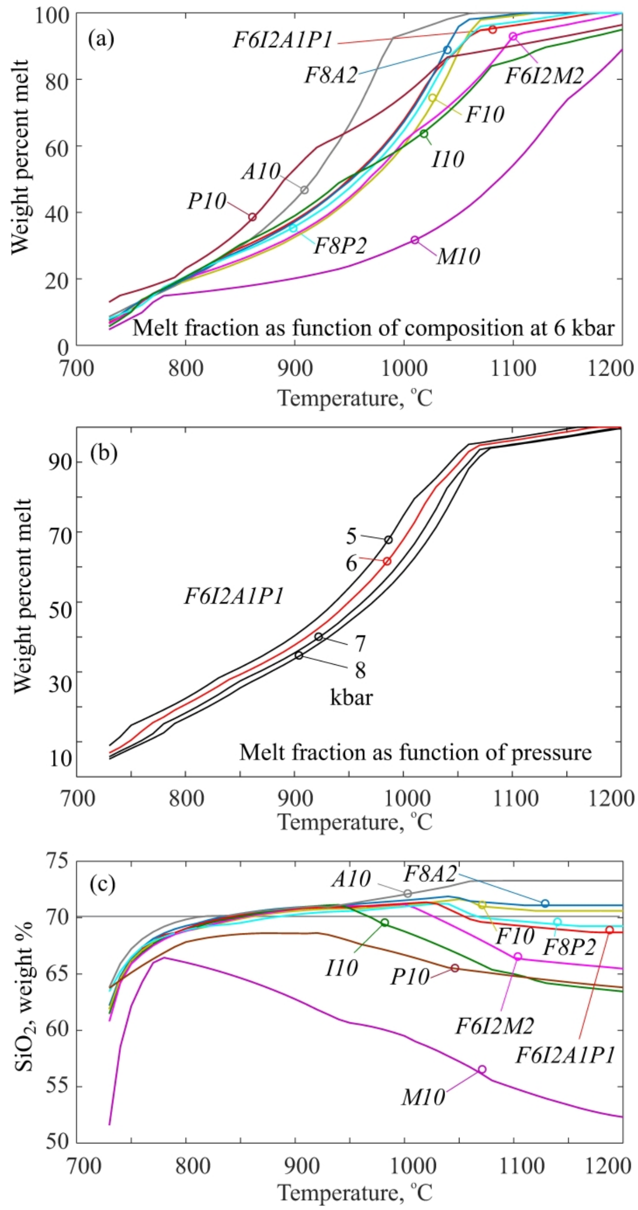

Figure 4

172x331mm (600 x 600 DPI)

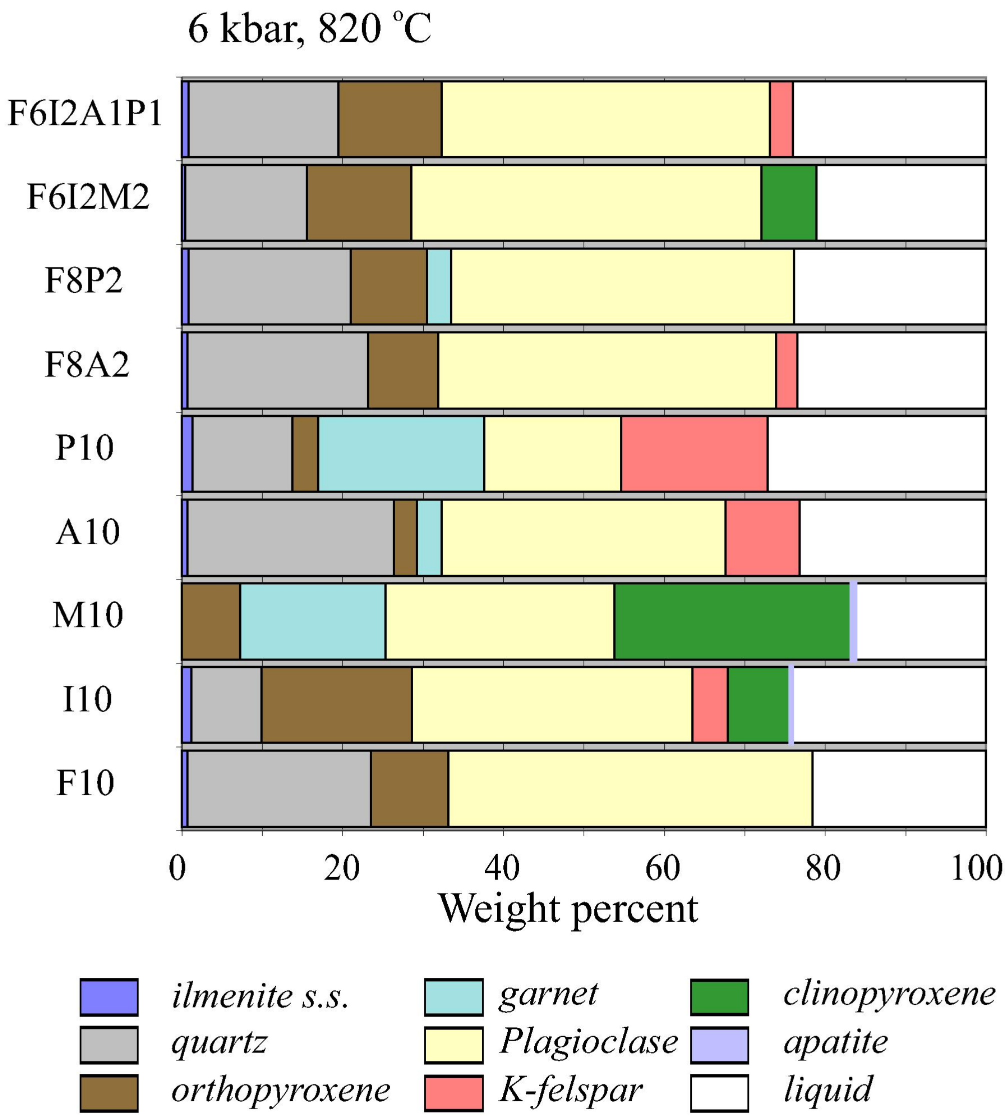

Fig. 6: Phase abundaces in weight percent at 6 kbar, 820 oC. Minor amounts of modal apatite are only present in bulk compositions M10 and I10.

75x83mm (600 x 600 DPI)

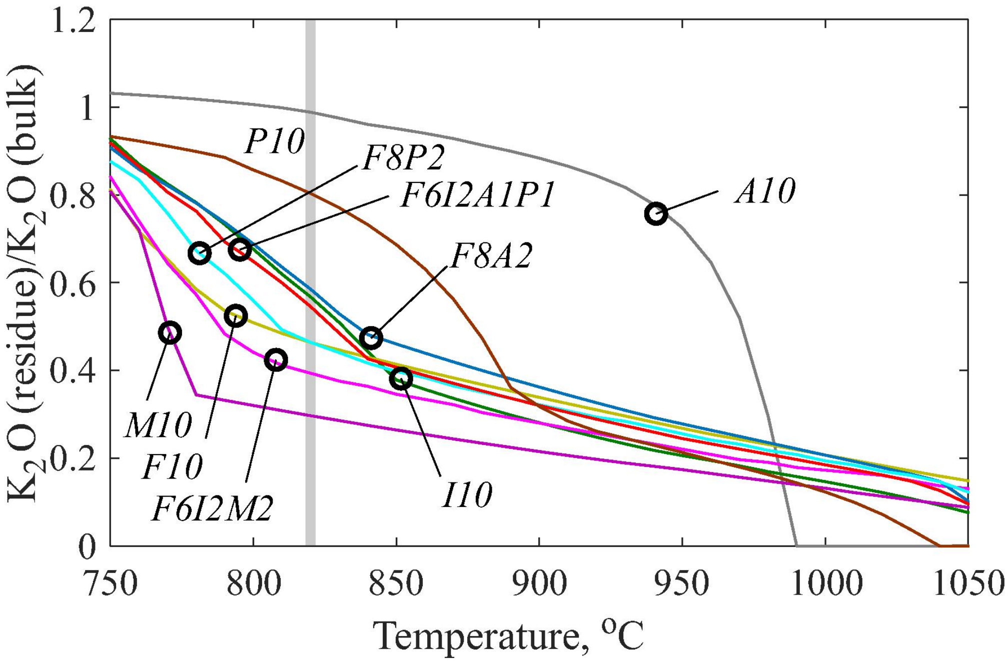

Fig. 7: Potassium depletion (as wt% K2O in residue / wt % K2O in total system. All residues are progressively depleted in potassium, except for the metaarkosite (A10) which shows a small increase in K2O below ca. 800 oC (i.e. the melt is less potassic than the residue in this temperature interval). The grey bar at 820 oC is shown to connect to the panels in Fig. 5.

75x49mm (600 x 600 DPI)

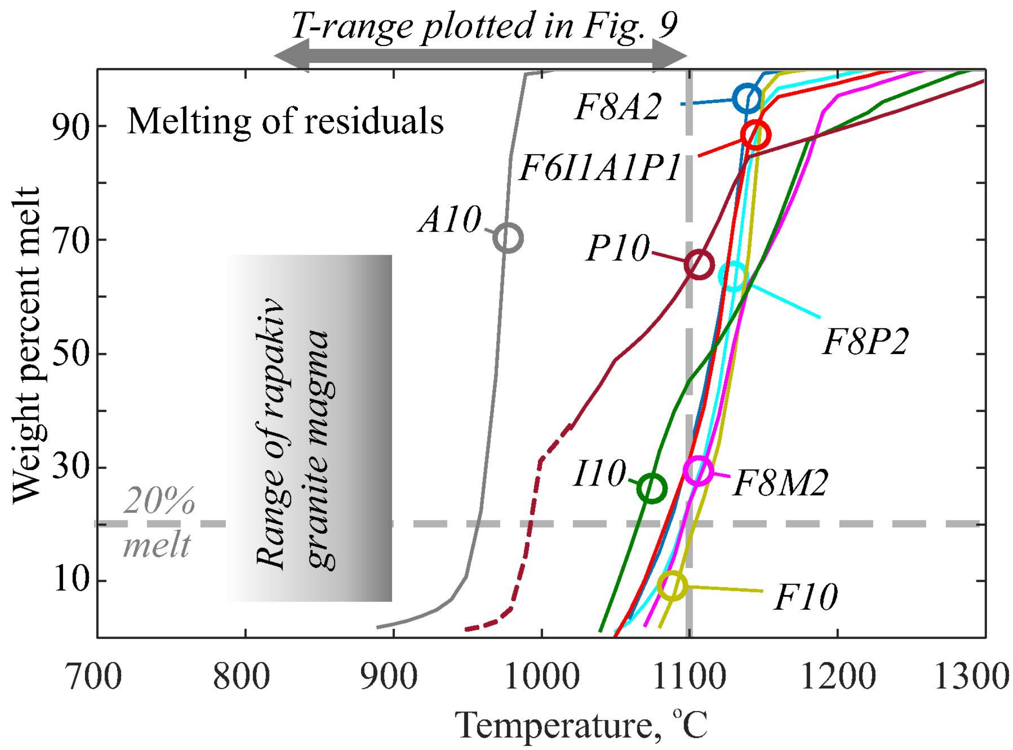

Fig. 8: Melt yields on further heating of melt-depleted residues formed at 6 kbar, 820 oC (assuming full separation of melt). All systems are anhydrous, but 100 ppm water was added to the metapelitic system (P10) at T<1020 oC to prevent software from malfunctioning (broken part of the curve).

75x55mm (600 x 600 DPI)

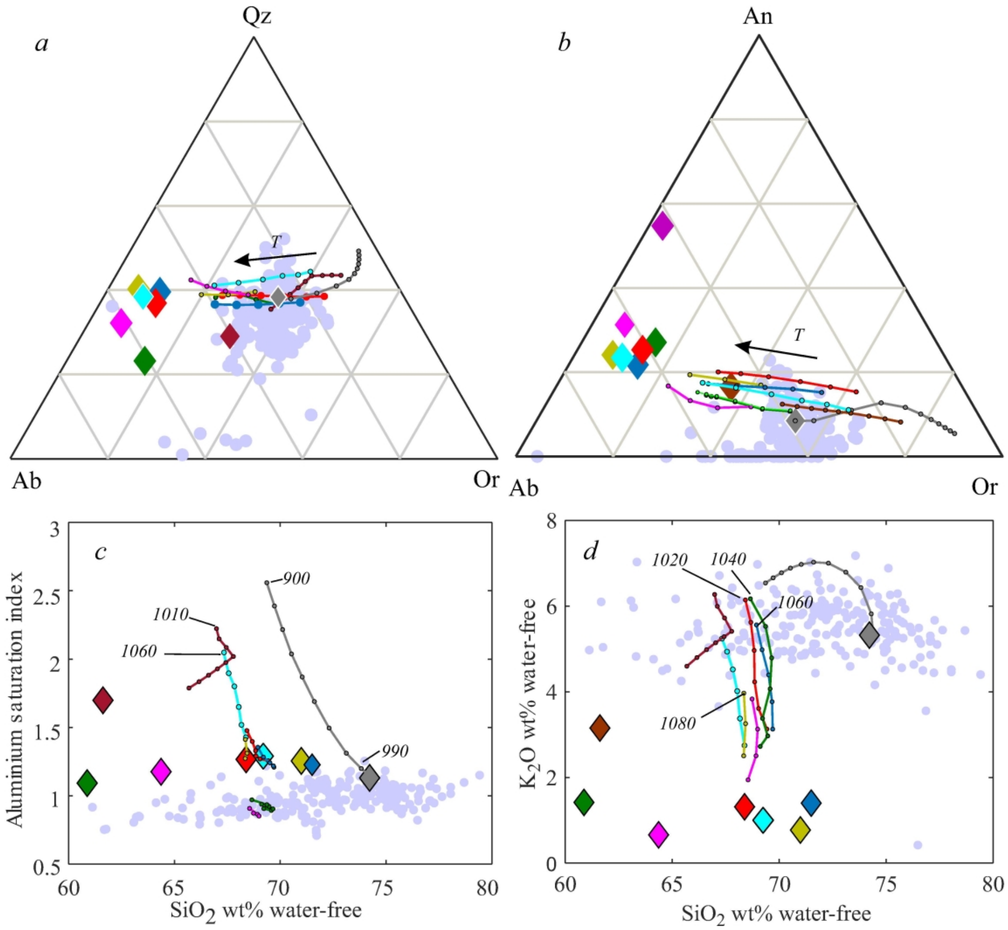

Fig. 9: Second generation melts obtained by further heating of the residues of the first melt separation at 820 oC, 6 kbar, compared to rapakivi granite compositions shown as grey background (panels and colour coding as in Fig. 5). Diamonds represent bulk composition of the residues, the evolution of melts are shown as lines terminating (at point closest to bulk composition) at 1100 oC, calculated at 10 degree intervals (indicated by tick marks). The starting temperature on the curves indicated on the curves differ among the bulk compositions, and reflect the temperature where a non-zero melt production is first seen (cf. Fig. 8), i.e. 900 oC for A10R, 1070 oC for F10R. Note that A10 is completely molten above 990 oC. Colour coding as in Fig. 5.

155x143mm (600 x 600 DPI)

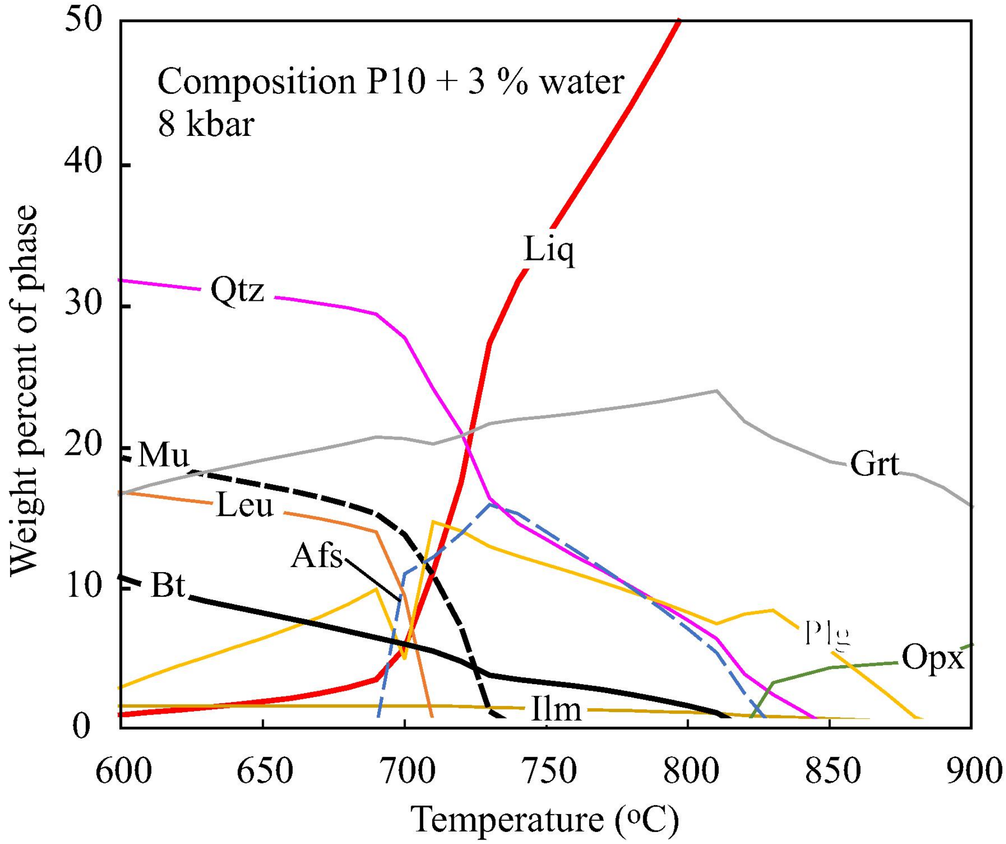

Fig. 10: Phase proportion in the low-temperature part of a numeric melting experiment of the P10 metapelite composition (Table 1) with 3% water at 8 kbar. Heavy curves give phase abundance of muscovite (Mu), biotite (Bi) and liquid (Liq) as function of temperature. Thin curves are other solid phases present in the restite (Ilm: Ilmenite, Afs: Alkali feldspar, Leu: Leucite, Qtz: Quartz, Plg: Plagioclase, Grt: Garnet, Opx: Orthopyroxene)

75x63mm (600 x 600 DPI)

Table 1. Source rock and unmelted residue compositions used in modelling (source rocks: Rock geochemical data of Finland, GTK 2020)

Initial compositions, weight percent oxides

	A10	P10	M10	I10	F10	F6I2M2	F8A2	F8P2	F6I2A1P1
SiO_2	73.1	63.0	51.6	62.5	70.4	65.1	70.9	68.9	68.4
TiO_2	0.4	0.8	1.2	0.8	0.4	0.6	0.4	0.5	0.5
Al_2O_3	12.7	16.8	15.8	13.2	13.8	14.1	13.6	14.4	13.9
Fe_2O_3	3.0	7.4	10.9	8.5	4.3	6.4	4.0	4.9	5.3
MnO	0.1	0.1	0.2	0.1	0.1	0.1	0.1	0.0	0.1
MgO	0.5	2.9	5.6	3.7	1.3	2.7	1.2	1.7	1.9
CaO	1.2	1.5	9.8	4.2	2.6	4.3	2.4	2.4	2.7
Na_2O	2.7	2.5	2.9	3.4	4.3	3.8	4.0	3.9	3.7
K_2O	5.4	3.9	0.9	2.5	1.7	1.7	2.4	2.1	2.4
P_2O_5	0.1	0.1	0.2	0.2	0.1	0.2	0.1	0.1	0.1
H_2O	1.0	1.0	1.0	1.0	1.0	1.0	1.0	1.0	1.0
	100.0	100.0	100.0	100.0	100.0	100.0	100.0	99.9	100.0

Residues (R) after melt-extraction at 6 kbar, 820 ^{o}C, weight percent oxides

	A10R	P10R	I10R	F10R	F6I2MR	F8A2R	F8P2R	F6I2A1P1R
SiO_2	74.0	61.1	60.8	70.7	63.9	71.2	68.9	68.0
TiO_2	0.4	0.9	0.9	0.4	0.7	0.4	0.5	0.5
Al_2O_3	12.5	16.5	13.2	13.9	14.2	13.7	14.1	13.9
Fe_2O_3	3.5	9.9	11.0	5.1	7.9	4.8	6.1	6.7
MnO	0.0	0.0	0.0	0.0	0.0	0.0	0.0	0.0
MgO	0.6	3.9	4.0	1.7	3.4	1.5	2.2	2.5
CaO	1.0	1.7	4.8	2.8	4.9	2.6	2.7	2.9
Na_2O	2.7	2.9	3.8	4.6	4.2	4.4	4.5	4.2
K_2O	5.3	3.1	1.4	0.8	0.7	1.4	1.0	1.3
P_2O_5	0.0	0.0	0.0	0.0	0.0	0.0	0.0	0.0
H_2O	0.0	0.0	0.0	0.0	0.0	0.0	0.0	0.0
	100.0	100.0	100.0	100.0	100.0	100.0	100.0	100.0

Key to the compositions:
A10 = Average arkosite, P10 = Average pelite, M10 = Average mafic metavolcanic rock, I10 = Average intermediate volcanic rock, F10 = Average felsic metavolcanic rock, F6I2M2 = 6:2:2 felsic + intermediate + mafic; F8A2 = 8:2 felsic + arkosite, F8P2 = 8:2 felsic + pelite, F6I2A1P1 = 6:2:1:1 felsic + intermediate + arkosite + pelite.